

## RESEARCH ARTICLE

# Maximizing sensitivity for fast GABA edited spectroscopy in the visual cortex at 7 T

Arjan D. Hendriks<sup>1</sup>  | Alessio Fracasso<sup>1,2</sup> | Catalina S. Arteaga de Castro<sup>1</sup>  |  
Mark W.J.M. Gosselink<sup>1</sup> | Peter R. Luijten<sup>1</sup> | Natalia Petridou<sup>1</sup> | Dennis W.J. Klomp<sup>1</sup>

<sup>1</sup>Department of Radiology, Imaging Division, University Medical Center Utrecht, Utrecht, The Netherlands

<sup>2</sup>Experimental Psychology, Helmholtz Institute, Utrecht University, Utrecht, The Netherlands

## Correspondence

Arjan D. Hendriks and Natalia Petridou, Department of Radiology, Imaging Division, University Medical Center Utrecht, Utrecht, The Netherlands.

Email: a.d.hendriks-6@umcutrecht.nl; n.petridou@umcutrecht.nl

## Funding information

Nederlandse Organisatie voor Wetenschappelijk Onderzoek, Grant/Award Number: Vidi Grant 13339 (Petridou)

The combination of functional MRI (fMRI) and MRS is a promising approach to relate BOLD imaging to neuronal metabolism, especially at high field strength. However, typical scan times for GABA edited spectroscopy are of the order of 6–30 min, which is long compared with functional changes observed with fMRI.

The aim of this study is to reduce scan time and increase GABA sensitivity for edited spectroscopy in the human visual cortex, by enlarging the volume of activated tissue in the primary visual cortex. A dedicated setup at 7 T for combined fMRI and GABA MRS is developed. This setup consists of a half volume multi-transmit coil with a large screen for visual cortex activation, two high density receive arrays and an optimized single-voxel MEGA-sLASER sequence with macromolecular suppression for signal acquisition.

The coil setup performance as well as the GABA measurement speed, SNR, and stability were evaluated. A 2.2-fold gain of the average SNR for GABA detection was obtained, as compared with a conventional 7 T setup. This was achieved by increasing the viewing angle of the participant with respect to the visual stimulus, thereby activating almost the entire primary visual cortex, allowing larger spectroscopy measurement volumes and resulting in an improved GABA SNR. Fewer than 16 signal averages, lasting 1 min 23 s in total, were needed for the GABA fit method to become stable, as demonstrated in three participants. The stability of the measurement setup was sufficient to detect GABA with an accuracy of 5%, as determined with a GABA phantom. *In vivo*, larger variations in GABA concentration are found: 14–25%. Overall, the results bring functional GABA detections at a temporal resolution closer to the physiological time scale of BOLD cortex activation.

## KEYWORDS

fast edited spectroscopy, fMRS, half volume coil, MEGA-sLASER, visual cortex,  $\gamma$ -aminobutyric acid (GABA)

**Abbreviations used:** Abs Diff, absolute difference; BOLD, blood oxygenation level dependent; cr, creatine; CRLB, Cramér-Rao lower bound; CV, coefficient of variation; EPI, echo-planar imaging; FID, free induction decay; fMRI, functional MRI; FOCI, frequency offset corrected inversion; GABA,  $\gamma$ -aminobutyric acid; IU, institutional units; MEGA-sLASER, Mescher-Garwood semi localized adiabatic selective refocusing; NAA, N-acetylaspartic acid; NSA, number of signal averages; ppm, parts per million ( $10^{-6}$ ); SD, standard deviation; SNR, signal-to-noise ratio; V1, primary visual cortex  
Natalia Petridou and Dennis W.J. Klomp are senior co-authors.

This is an open access article under the terms of the Creative Commons Attribution-NonCommercial License, which permits use, distribution and reproduction in any medium, provided the original work is properly cited and is not used for commercial purposes.

© 2018 The Authors. *NMR in Biomedicine* published by John Wiley & Sons Ltd.

## 1 | INTRODUCTION

Blood-oxygenation-level-dependent (BOLD) functional MRI (fMRI) is the most widely used technique to measure brain function non-invasively in humans. BOLD measurements capture neuronal activity indirectly, via changes in blood flow, volume, and oxygenation.<sup>1,2</sup> These changes arise from local changes in neuronal activity and metabolism. The relationship between BOLD signals and excitatory neuro-metabolic processes has been studied extensively; however, the relationship between BOLD signals and inhibitory neuro-metabolic processes is less well understood.<sup>3-5</sup> One of the key inhibitory metabolites is  $\gamma$ -aminobutyric acid (GABA), which is the main inhibitory neurotransmitter of the brain and is believed to have a direct impact on BOLD contrast through regulation of neuronal firing rates.<sup>6-8</sup> In the human brain *in vivo*, the relationship between GABA and BOLD signals has been investigated in studies that combined fMRI and MRS.<sup>7,9-15</sup>

Edited GABA spectroscopy is a commonly used technique to measure GABA levels.<sup>16</sup> With edited spectroscopy it is possible to separate the GABA signal from the signal of other metabolites. Faster non-edited, short echo time MRS techniques have been used for functional measurements of other metabolites as well, but often lack reliable quantification of GABA, because of contamination from overlapping resonances.<sup>17</sup>

In order to further relate BOLD signal to GABA, it is desirable to measure GABA changes within the time scale of BOLD changes, meaning short scan times. Short scan times enable the measurement of rapid changes in GABA levels that are induced by specific cognitive tasks carried out by the participant inside the scanner.<sup>9,12,18</sup> Typical scan times for GABA edited spectroscopy reported in literature are of the order of 6-30 min,<sup>16</sup> which is impermissibly long when compared with functional changes observed with fMRI. To further reduce scan time of GABA edited spectroscopy, the measurement method needs to be highly sensitive to GABA, allowing reduction of scan time per measurement.

At high magnetic field strengths, such as 7 T or higher, the combination of BOLD fMRI and GABA MRS is particularly promising, because both BOLD contrast and MRS sensitivity are enhanced. This gain in sensitivity at high field can be traded for shorter measurement times. Nevertheless, even at high field, the sensitivity for functional GABA edited spectroscopy might not be enough. A seemingly simple solution to increase spectroscopic sensitivity is to increase the voxel size. However, when interested in specific regions of the brain, or regions that only contain tissue stimulated by a task, the voxel size must be limited by the corresponding physical brain shapes or by the maximal regional extent of stimulated tissue.

The aim of this study is to reduce scan time and increase GABA sensitivity for edited spectroscopy in the visual cortex. To realize this aim, a dedicated coil setup high field strength (7 T) MRI scanner was developed with a large projection screen. We focus on the visual cortex, because it is well characterized and it can be stimulated in a well-controlled manner. The developed setup consists of a multi-transmit head coil and high density receive arrays. The setup is developed for combined fMRI and GABA MRS at 7 T in the visual cortex. The setup facilitates a clear visual view to a large screen, enabling a wide radial visual stimulus with a large visual angle. We expect that a stimulus with a large visual angle can activate a large cortical volume, which enables a large voxel size for spectroscopy, resulting in an enhanced GABA signal-to-noise ratio (SNR). GABA measurements are performed with a MEGA-sLASER (Mescher-Garwood semi localized adiabatic selective refocusing) sequence with macromolecular nulling. The sequence is modified to include frequency offset corrected inversion (FOCI) editing pulses, enhancing GABA detection and spatial localization.<sup>19</sup> This setup enabled us to measure individual GABA concentrations over a short period of time. The effectiveness of the approach to achieve short scan time is evaluated in two steps. First, the coil setup performance with visual stimulus is assessed, by mapping the extent of activation in primary visual cortex (V1), and by determining the corresponding increase in spectroscopy voxel size. Second, the achievable SNR, speed and stability of the GABA measurements are assessed by performing multiple repetitive GABA measurements in the same region.

## 2 | DESIGN

### 2.1 | Coil setup and MRS sequence design, rationale

Three important aspects were taken into account for the design of the setup. First, the size of the projected visual stimulus, and corresponding visual angle of view of the subject, directly influences the size of visual cortex tissue volume that can be activated.<sup>20</sup> An increased visual angle of view of the participant, for example due to an increased screen size, leads to activation of a greater part of the visual cortex. When measuring GABA in this greater part of the visual cortex, the acquisition volume (size of the single voxel) can be increased, which in turn delivers a stronger GABA signal with an enhanced SNR. The gain in GABA SNR can be used to reduce the GABA spectroscopy acquisition time. As an additional advantage, by increasing the amount of stimulated tissue, the interference of signals arising from non-stimulated tissue can also be minimized. At high field, the elongated scanner bore together with closed transmit coil configurations decreases the maximum projection size for visual stimulation. Often, multiple mirrors and prisms have to be used, at the cost of reducing the participant's visual angle. Half volume multi-transmit coils that are specialized for the visual cortex do not have this drawback, and have recently been shown as a promising research tool for functional imaging.<sup>21</sup> The concept of an open half volume coil design<sup>22-27</sup> is used in this study to construct a setup that enables visual stimulation with a large visual angle.

Second,  $B_1$  field uniformity over the acquisition volume is needed to reach the desired flip angle, which is especially important for GABA spectroscopy, in which editing pulses assume a uniform  $B_1$  field. Using multiple RF transmit coil elements in parallel can significantly improve  $B_1$  field uniformity of high field MRI.<sup>28</sup> Therefore, the half volume coil was built with multiple channels for RF transmission to optimize  $B_1$  uniformity.

Third, an optimized MEGA-sLASER sequence was implemented for enhanced GABA detection.<sup>29</sup> The sequence includes macromolecular nulling to minimize the contamination of the GABA signal by macromolecules. To optimize sequence performance, we employed FOCI pulses as

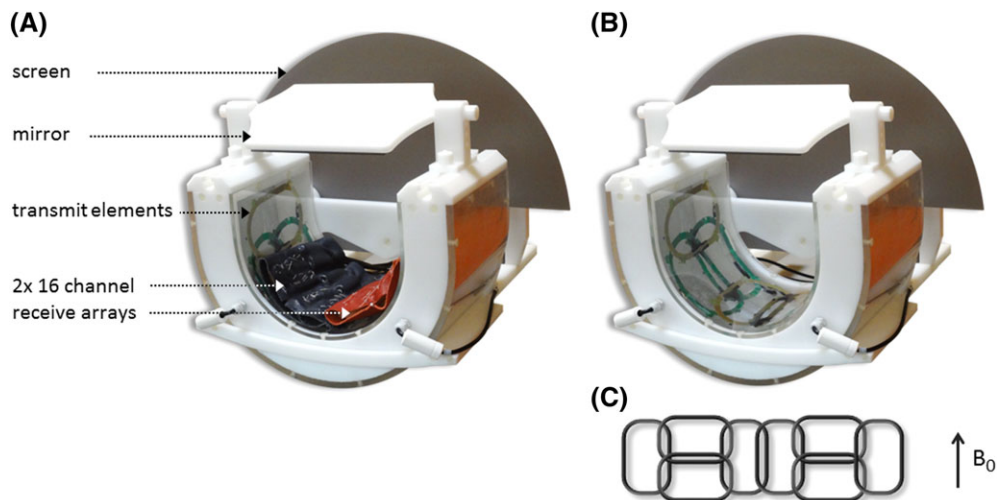


**FIGURE 1** Overview of the half volume coil setup. The transmit coil is open (U shaped), allowing a visual stimulation with fewer mirrors and a large visual angle. (A), A photograph of the coil setup, in which the main components are labeled, including the 16-channel receive arrays; (B), a photograph of the coil setup without the receive arrays in place, showing the actual transmit elements; (C), the transmit element arrangement in a schematic flat view, to illustrate the positions of the eight transmit elements relative to each other in more detail

a means to increase the bandwidth of adiabatic pulses,<sup>19</sup> reducing chemical shift displacement artifacts, and thus improving the spatial localization of GABA signals.

## 2.2 | Coil setup specifications

A dedicated coil setup was constructed for a 7 T MR system (Philips, Best, The Netherlands). The setup (Figure 1) consists of a shielded open half-cylinder multi-transmit head coil with eight transmit elements. The eight transmit elements are oval shaped, with a size of  $16 \times 10 \text{ cm}^2$ , facilitating  $B_1^+$  shimming in three dimensions. Each element is matched to  $50 \Omega$  at 298 MHz when loaded with the participant's head. The transmit elements are arranged on the half cylinder with their direction towards the back of the head (Figure 1B). Four elements are aligned along the direction of the  $B_0$  field and two pairs of two elements orthogonal to the field (Figure 1C). To maximize inductive decoupling of the elements with their nearest neighbors, all elements are positioned with a partial overlap of their adjacent elements. The overlap was determined by minimizing the  $S_{12}$  coupling in pairs, beginning with the center two elements followed by the paired orthogonal elements. This was done separately for each pair, without the other elements present. Subsequently, the overlap of the two orthogonal pairs with the center pair of elements was optimized by minimizing the  $S_{12}$  coupling between the pairs. Finally, the outer two elements were positioned with an overlap of the orthogonal pairs of elements such that  $S_{12}$  between the outer and the neighboring pair of elements was minimized. The elements are made of printed circuit board material and incorporate PIN diodes for detuning during receive. The RF coils are all actively detuned. The transmit elements are detuned during the receive phase and the receiver coils during the transmit phase. The elements are embedded in plexiglass. The surrounding U-shaped casing is custom made out of 6 mm thick polyoxymethylene, while aluminum foil was used as RF shielding to prevent coupling to the cables and conductors in the patient bed. The transmit elements are connected to two 4 kW and six 1 kW amplifiers via ceramic cable traps tuned to 298 MHz and transmit-receive switches. The amplifiers can be controlled in amplitude and phase for RF shimming over the visual cortex with a target  $B_1^+$  of  $20 \mu\text{T}$ .

A projection screen, with bars of adjustable length embedded in the coil casing, is mounted at the back of the coil. The screen size is 35 cm high by 56 cm wide, just small enough to fit in the scanner bore. A  $17 \times 20 \text{ cm}^2$  mirror is mounted on top of the coil casing on sliding bars that can be used to adjust the mirror location with respect to the participant's eyes (Figure 1A,B). Using back-projection of visual stimuli, the size of the projection achieved is  $17 \times 24 \text{ cm}^2$ . The mirror can be positioned approximately 10 cm from the participant's eyes and angled at  $45^\circ$ , resulting in a visual angle of more than  $60^\circ$ .

The receive part of the setup consists of two high density 16-channel surface arrays (MR Coils, Zaltbommel, The Netherlands). The high density receive arrays with small coil elements fit tightly on the participant's head, and are used to produce high resolution, high SNR, fMRI and MRI scans, with a receive depth extending several centimeters from the coil elements.<sup>30,31</sup>

## 2.3 | Reference setup specifications

The performance of the custom-made coil setup was examined relative to the standard head coil setup of our 7 T system. The standard setup consists of a dual-channel volume transmit coil in combination with a 32-channel receive head coil<sup>32</sup> (Nova Medical, MA, USA). The projection screen for the standard setup at our site is located at the front of the transmit coil and is visible through prism glasses and a mirror approximately 30 cm from the participant's eyes (see Figure 2A later). Using back-projection of visual stimuli the projection size achieved is  $9 \times 15 \text{ cm}^2$ , yielding a visual angle of approximately  $11^\circ$ .

## 3 | METHODS

The half volume coil setup was evaluated in two steps. First, the coil setup performance was evaluated by performing GABA measurements in four participants and fMRI in one participant, focusing on the spatial extent of visual cortex activation and corresponding maximal achievable size of the GABA voxel. These results were evaluated relative to the standard head coil setup of our 7 T system. Second, the SNR, speed, and stability of the GABA measurements were assessed by carrying out multiple repetitive measurements with the half volume coil setup in three participants at rest and in a phantom. All participants gave informed consent, and the work was approved by the Medical Ethics Committee of the University Medical Center Utrecht.

### Preparation and shimming

Before acquiring the fMRI and GABA scans, a number of preparation steps were performed. A  $T_1$ -weighted scan was acquired for both setups as anatomical reference (3D gradient echo,  $T_E/T_R = 2.1/4.5$  ms, flip angle  $5^\circ$ ,  $2 \times 2 \times 2$  mm<sup>3</sup> voxel size,  $250 \times 250 \times 198$  mm<sup>3</sup> FOV, 99 sagittal slices, and a duration of 1 min). For the half volume setup, an extra preparation phase was performed to shim the  $B_1$  field on V1 based on eight low flip angle gradient echo image series obtained by driving a different transmit element each time (multi-slice gradient echo series, with a  $T_E/T_R$  of 0.85/15 ms, flip angle  $10^\circ$ ,  $3.9 \times 3.9 \times 10$  mm<sup>3</sup> voxel size,  $190 \times 221 \times 70$  mm<sup>3</sup> FOV, seven slices, and a duration of 7 s). The resulting  $B_1^+$  level was assessed with a  $B_1$  map (AFI,<sup>33</sup> 3D gradient echo,  $T_E/T_R = 2.2/25$  ms, flip angle  $50^\circ$ ,  $3 \times 3 \times 3$  mm<sup>3</sup> voxel size,  $176 \times 220 \times 27$  mm<sup>3</sup> FOV, nine slices, and a duration of 1 min 47 s). The  $B_1$  shimming procedure was performed for each participant individually and lasted around 10 min in total.  $B_1$  shimming was not performed with the standard head coil. As the final preparation step for both coil setups, a  $B_0$  map of the posterior part of the brain was acquired, which was used for third order  $B_0$  phase map shimming ( $B_0$  map, 3D gradient echo,  $T_E/T_R = 1.96/4.7$  ms, flip angle  $10^\circ$ ,  $2 \times 2 \times 2$  mm<sup>3</sup> voxel size,  $190 \times 190 \times 70$  mm<sup>3</sup> FOV, 35 coronal slices, and a duration of 1 min). The linewidth of the water peak after  $B_0$  shimming measured in the respective voxel, was on average  $14 \pm 1$  Hz (mean  $\pm$  SD) for the half volume coil setup and  $15 \pm 2$  Hz for the standard setup.

### 3.1 | Coil setup performance

The coil setup performance was evaluated in terms of spatial extent of visual cortex activation assessed with fMRI and corresponding maximal achievable voxel size and SNR for GABA MRS measurements. The performance of the custom-made coil setup was examined relative to the standard head coil setup of our 7 T system. For the coil setup comparison, four participants were scanned with both setups. Three participants were scanned with three GABA edited MRS scans of 5 min 30 s each (no fMRI). One participant was scanned with both fMRI and two GABA edited MRS scans of 5 min 30 s.

#### fMRI acquisition

Visual stimuli consisted of a contrast-reversing checkerboard at 6 Hz, presented at full visual field to assess the spatial extent of activation in V1. The participant was instructed to fixate the eyes on a central cross. The projection size was maximized according to the setup used. Full visual stimuli were presented in a block design with the contrast-reversing checkerboard 7 s on/18 s off. The duration of each run was 3.5 min. fMRI data were acquired using single-shot echo-planar imaging (EPI), with  $T_E/T_R = 27/1800$  ms, flip angle  $60^\circ$ ,  $1.5 \times 1.5 \times 1.5$  mm<sup>3</sup> voxel size,  $160 \times 170 \times 53$  mm<sup>3</sup> FOV, and 35 slices orthogonal to the calcarine sulcus (Figure 2D later).

#### fMRI analysis

fMRI data were analyzed using AFNI.<sup>34</sup> Data were corrected for motion and drift, and active voxels were identified with correlation of the stimulus waveform convolved with the canonical hemodynamic response. Activation maps were obtained by thresholding the resulting correlation coefficient maps at  $p < 10^{-5}$  uncorrected. The comparison between the activation maps of the two coils was performed by visual inspection of the spatial extent of activity in V1. To quantify the difference, an ROI analysis was performed as follows. The mean EPI image was computed for each fMRI time series, i.e. for each coil. A transformation matrix was obtained by co-registering the mean EPI images of the half volume coil to the mean EPI image of the head coil using AFNI (3dWarpdrive function, rigid body transformation). This transformation matrix was applied to the correlation coefficient maps obtained for the half volume coil data (3dAllineate function), bringing the activation maps of both coils into the same space. An ROI was selected on the mean EPI image of the head coil, encompassing that part of the visual cortex that corresponds to the large MRS voxel. Inside the ROI, the number of significantly active voxels was counted and compared between setups.

#### MRS acquisition

A single voxel was positioned to approximately encompass the active regions in V1 in both hemispheres. GABA edited spectroscopy was performed using a MEGA-sLASER sequence. For each participant, consecutive MRS scans were performed during one scanning session with the half volume coil setup; the session was repeated on a different day using the standard head coil setup. Three participants were scanned with three GABA edited MRS scans for both receive setups. The MRS acquisition parameters used for these three participants were  $T_E/T_R = 74/5000$  ms, spectral bandwidth 4000 Hz, 32 odd/even pairs, number of signal averages (NSA) 64 and a total acquisition time of 5 min 30 s. The voxel size for the standard setup was  $25 \times 25 \times 20$  mm<sup>3</sup>, and for the custom half volume coil setup  $40 \times 30 \times 30$  mm<sup>3</sup>. Besides these three participants, one additional participant was scanned with both fMRI and two MRS scans, where the generic voxel size and location of the MRS scan was adapted to match directly to the activation area observed with fMRI. The same MRS acquisition parameters were used as described above, except for a voxel size for the half volume coil setup of  $40 \times 40 \times 20$  mm<sup>3</sup>,

approximately spanning the fMRI activation maps (Figure 2C,E,F,G later). The MEGA-sLASER sequence combined two dual-banded editing pulses applied alternatively in odd/even acquisitions, to suppress the macromolecules and water signals simultaneously, while refocusing the 3.0 parts per million (ppm) GABA signal.<sup>29</sup> FOCI pulses were implemented to increase the bandwidth of the adiabatic pulses.<sup>19</sup> Note that for a MEGA-sLASER sequence the acquisition of one editing pair consists of one odd and one even spectrum, acquired over a period of two  $T_R$  intervals, which is counted as two signal averages. In addition to the water suppression of the two dual-banded editing pulses, VAPOR was applied with a window of 250 Hz. To also measure the water signal, each scan was preceded by an unsuppressed water pre-scan. No visual stimulation was applied for the MRS measurements.

### MRS data processing

The spectra were processed using MATLAB (8.3, MathWorks, MA, USA). The processing steps performed were phasing and apodization (10 Hz), residual water removal by HLSVD fitting,<sup>35</sup> retrospective frequency and phase alignment of the acquired NSA based on the choline and creatine signal,<sup>36,37</sup> and last adding the odd/even spectra, resulting in an edited GABA spectrum.<sup>29</sup> Afterwards, the edited spectra were fitted to estimate the relative concentration of GABA and creatine (as a reference). The fit procedure was implemented in the same MATLAB routine as the data processing steps. Fitting of the metabolite peaks was performed with an iterative Lorentzian fitting function, regulating peak amplitude, linewidth, frequency, and offset (zeroth order baseline). For GABA, a double Lorentzian curve was fitted at 3.0 ppm with 14 Hz peak splitting. The creatine signal was fitted in the metabolite spectrum (odd and even subtracted). This was done as a reference, and as validation of the editing procedure. Both the area under the metabolite peak and the Cramér-Rao lower bound (CRLB) were estimated in the fitting procedure. Reported SNR values were calculated in the time domain (free induction decay, FID), by dividing the signal amplitude of the fitted metabolite (GABA or creatine) in the time domain by the standard deviation (SD) of the noise at the end (last 15%) of the acquired FID signal. This is done to obtain a metric for SNR that is independent of line shape.<sup>38</sup> SNR was calculated for both coil setups; as spectral resolution of the GABA resonance was similar for both setups, the SNR gain was quantified as the ratio of the two SNR values.

## 3.2 | SNR, speed, and stability of the GABA measurements

The SNR and stability of GABA measurements using the custom coil setup was assessed in three healthy volunteers and a phantom. The minimum achievable scan time with the coil setup was assessed by the number of averages required to reach a stable fit of the GABA peak, given by the number of averages required for the CRLB of the fit algorithm to reach a plateau. The stability of the GABA measurements was assessed by bootstrapping sets of spectra and computing the variance of the fitted GABA peak. The detection limits of the measurement and accuracy of the fit procedure were evaluated on a phantom.

### Acquired spectra

MRS measurements were made in three participants with a MEGA-sLASER sequence of 5 min 30 s and a voxel size of  $40 \times 30 \times 30 \text{ mm}^3$ . The parameters of the MEGA-sLASER sequence were the same as described above in the methods for the coil setup performance. The measurement was repeated three times per participant.

Additionally, phantom measurements were made. The phantom consisted of a 4 cm diameter ping-pong ball containing the metabolites GABA and creatine. A phantom with a small diameter was chosen, to avoid artifacts originating from standing waves. Standing waves can appear because the RF wavelength at a field strength of 7 Tesla is smaller in a phantom than *in vivo* due to their dielectric differences. Because of the small diameter of the ball, the voxel size that could be fitted inside the volume of the phantom was six times smaller than that employed for the *in vivo* measurements. To compensate for this difference in voxel size, a six times higher concentration was chosen for the metabolites in the phantom (GABA 6.6mM, creatine 48mM) than assumed *in vivo*, matching the SNR between the phantom and *in vivo* measurements. The MEGA-sLASER sequence parameters were the same as for the *in vivo* measurements, except for a voxel size of  $17 \times 20 \times 17 \text{ mm}^3$ . The measurement was repeated six times. Processing and fitting of the spectra was the same as described above in the methods of the coil setup performance. However, in the phantom no choline was present; therefore, in the processing steps, alignment was based on the creatine signal only.

### SNR and speed

To assess the minimum achievable scan time for a stable fit of the GABA peak, the NSA was incrementally increased and fitted. The area under the metabolite peak and the CRLB were estimated in the fitting procedure. The number of spectra that were averaged increased incrementally in steps of two, from two to 64 (the entire scan), and the CRLB and SNR were computed at each step. The CRLB was calculated according to Cavassila et al.<sup>39</sup> The minimum achievable scan time (speed) was assessed by the number of spectra required for the CRLB of the fit algorithm to reach a plateau. For the data in this study, the plateau was defined as a rate of GABA CRLB decay of less than 10% for all participants.

### Stability

To assess the GABA variation over a short period of time, a bootstrapping procedure<sup>40</sup> was employed. Bootstrapping was the preferred method, since the GABA peak was difficult to distinguish from noise for the spectrum obtained from one pair of edited data acquisition (NSA 2). With the bootstrapping procedure, an estimate could be obtained for the error and variance of GABA over a short period of time. In the bootstrap procedure, 500 random pairwise combinations of 16 signal averages (eight pairs) were selected out of a total of 64 (32 pairs). Consecutive odd/even

acquisitions were kept together (per pair) during the randomization. Each selected combination was added and fitted, resulting in 500 fits of the GABA and creatine peaks. The procedure was repeated to also bootstrap 32 signal averages out of 64. The mean and SD of the metabolite peak areas were calculated over the 500 fits (all bootstraps) to obtain an estimate for the error and variance of the metabolite peaks over a short period of time. Since the concentrations of the metabolites in the phantom do not change over time, the stability of the measurement method could be determined by applying the same procedure to the phantom measurements.

## 4 | RESULTS

### 4.1 | Coil setup performance

Figure 2A,B shows the standard 32-channel head coil setup and half volume coil setup respectively. The shaded (Figure 2A) and illuminated (Figure 2B) parts of the projection screen give an estimate of the difference in visual field of view between the two setups. The visual field of view

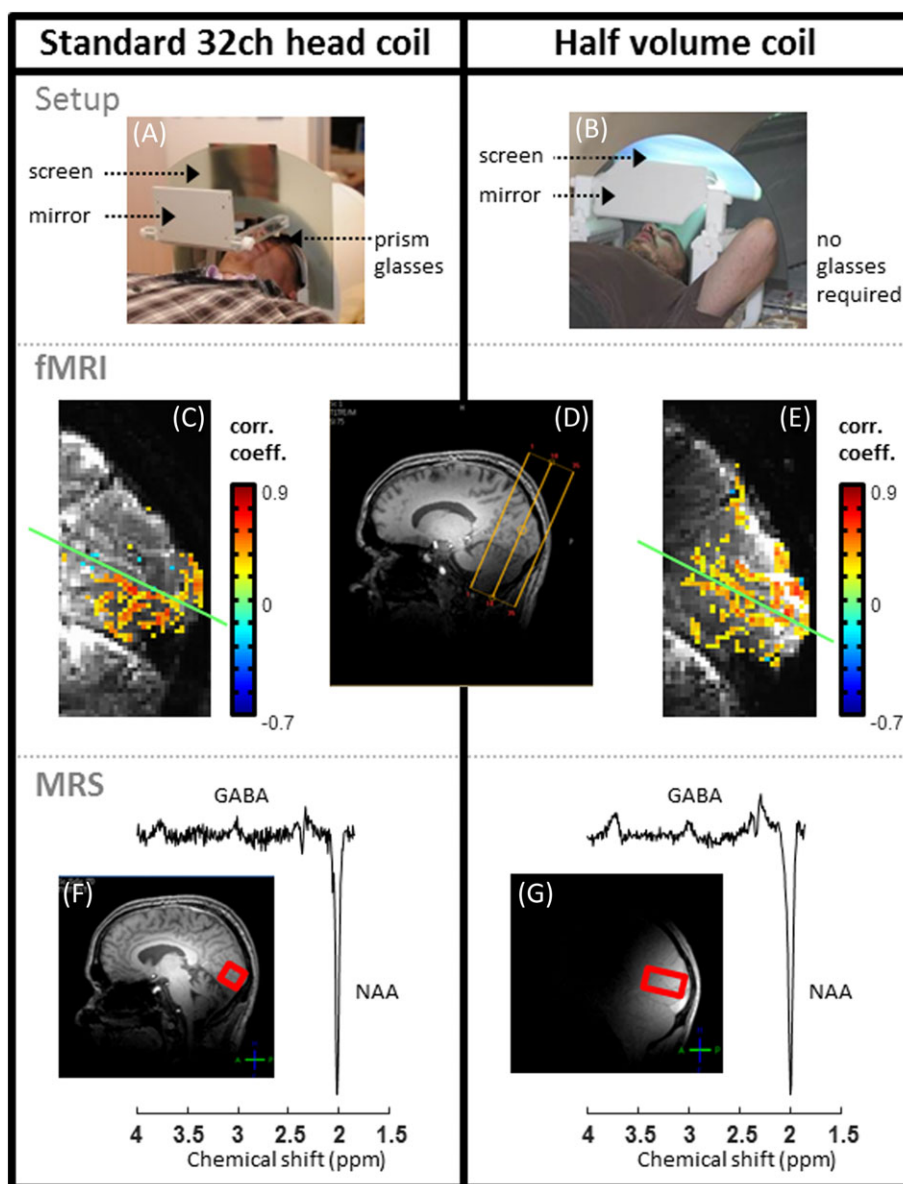


**FIGURE 2** Coil setup comparison of one participant. As reference, the standard 32-channel head coil (A), was used to compare with the half volume coil (B). Both setups have a mounted screen for visual stimulation. The maximum visual field of view achieved with the setups (A,B) directly influences the extent of visual cortex activation (C,E) as measured with fMRI. The fMRI activation map (correlation coefficient,  $p < 10^{-5}$  uncorrected) is overlaid on a sagittal view of the mean image of the EPI time series. (D) The position of the fMRI scan is indicated on a T1-weighted anatomical scan. (C,E), There is an increase in the extent of activation in the fMRI maps for the half volume coil setup, especially in the superior-inferior direction. The added green lines mark the calcarine, specifically separating the upper and lower banks. (F,G), The increase in activated tissue allows for a larger spectroscopy voxel of  $40 \times 40 \times 20 \text{ mm}^3$  (G), as compared with the voxel of the reference setup of  $25 \times 25 \times 20 \text{ mm}^3$  (F). The larger voxel size yields an SNR improvement of the GABA measurement, as can be seen in the two spectra. Both spectra consist of 16 signal averages and are acquired in 1 min 23 s

achieved with the standard 32-channel head coil (Figure 2A) gives rise to activation in a part of V1, as measured with fMRI (Figure 2C). The large visual field of view achieved with the half volume coil setup (Figure 2B) enabled a larger activation encompassing approximately the whole extent of V1 (Figure 2E). The spatial extent of activation was larger than that obtained with the standard head coil, most notably in the upper part of V1 (upper bank of the calcarine sulcus) due to the elongated screen height (Figure 2C,E). The increased spatial extent of activity allowed for a 2.5 times larger MRS voxel size comprising tissue that would be uniformly stimulated (Figure 2F,G). The benefits of the increased voxel size obtained with the new setup can be seen in the MRS spectra by a substantial increase in SNR.

Quantification of the increase in spatial extent of tissue activation and the increase in GABA SNR can be found in Table 1 and 2, respectively. The spatial extent of tissue activation was quantified as the number of active voxels in an ROI of the same size as the large MRS voxel. As can be seen in Table 1, the spatial extent of tissue activation for the half volume coil setup increased by approximately 19%, as compared with the standard 32-channel head coil. The GABA SNR was measured in four participants and the values can be found in Table 2. For the half volume coil setup, there is an increase in GABA SNR in all participants. The increase in GABA SNR varies per participant and is not directly equal to the increase in voxel size. Overall, the average increase in GABA SNR of the half volume coil over all participants is a factor of 2.2, as compared with the standard 32-channel head coil.

The resulting  $B_1^+$  map obtained after shimming over the visual cortex is shown in Figure 3. Note that a  $B_1^+$  of around 16  $\mu\text{T}$  could be obtained in the visual cortex, despite the absence of transmit elements on the upper part of the head.

## 4.2 | SNR, speed, and stability of the GABA measurements

### Acquired spectra

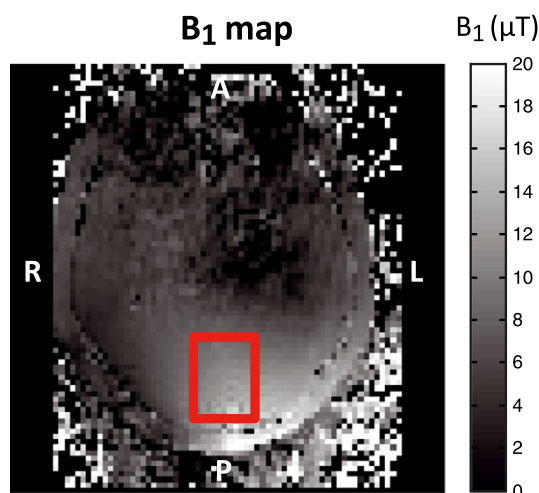
As an initial step, the quality of the acquired spectra was evaluated by visual inspection. Figure 4 shows an example of the acquired spectra after processing (phasing, apodization, alignment, addition of odd/even acquisitions) for the three participants, indicated in blue, green, and red respectively. Figure 4

**TABLE 1** fMRI comparison between the two setups. The number of active voxels was counted in an ROI of equal position and size as the large MRS voxel

Reference setup (n)	Half volume coil (n)	Increase (%)
2470	2947	19

**TABLE 2** GABA SNR comparison between the two setups

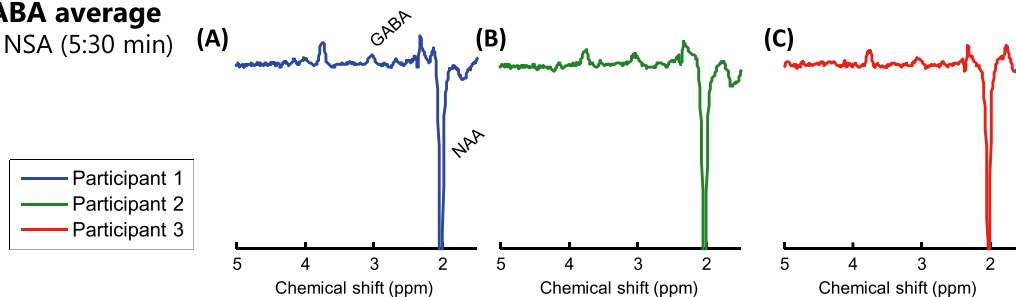
Participant no	MRS scans per setup (n)	GABA SNR (mean $\pm$ SD)		SNR increase, factor	Voxel size increase, factor
		Reference setup	Half volume coil		
1	3	2.0 $\pm$ 0.2	3.2 $\pm$ 0.6	1.6	2.88
2	3	1.5 $\pm$ 0.5	4.5 $\pm$ 0.9	3.0	2.88
3	3	1.1 $\pm$ 0.2	2.6 $\pm$ 0.5	2.4	2.88
4	2	2.3 $\pm$ 0.5	5.1 $\pm$ 0.4	2.2	2.56
All	11	1.7 $\pm$ 0.6	3.7 $\pm$ 1.1	2.2	2.8



**FIGURE 3** A  $B_1$  map acquired with the half volume coil. Beforehand, the  $B_1$  field is shimmed for optimal performance in the back of the head, with a  $B_1$  value of around 16  $\mu\text{T}$ . The size and position of the GABA voxel is also indicated (red square)

**GABA average**

64 NSA (5:30 min)

**GABA over time**

16 NSA (1:23 min)

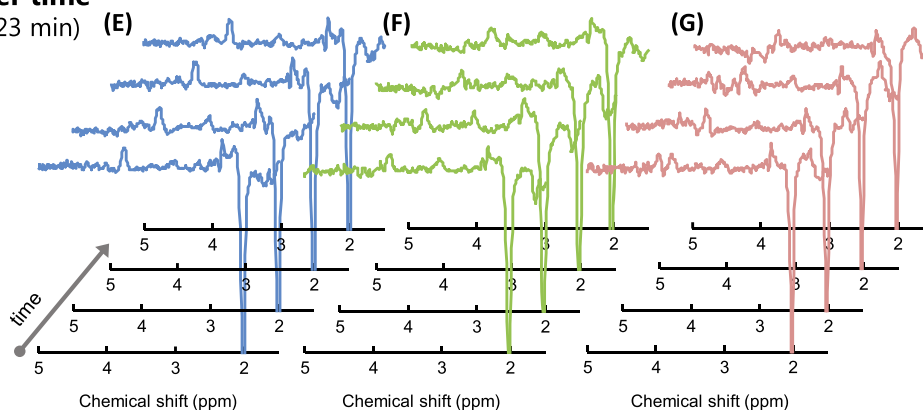


**FIGURE 4** Illustration of the acquired GABA edited spectra after processing. (A-C), one scan consisting of 64 signal averages is shown for all three participants (blue, green, red). At 3.0 ppm the GABA peak is clearly visible. (C-E), Each spectrum is split into four sets of 16 signal averages, to also inspect the temporal behavior of the GABA peak within one scan. Even though these spectra consist of only 16 signal averages and are thus noisier, the GABA peak can still be distinguished

A-C shows the edited spectra for one scan per participant. For each scan 64 signal averages are acquired. Note that the GABA peak is clearly visible in the spectra of all three participants. To get an impression of the temporal fluctuation within these 64 signal averages, the data of each participant was split into four sets of 16 signal averages, which are shown in Figure 4E-G. These spectra appear noisier since they were computed from only 16 signal averages. Still, the GABA peak can be distinguished in the spectrum, though small differences in GABA peak area are hard to evaluate visually from these plots.

**SNR and speed**

The analysis of the fitted spectral data of the phantom and the three different participants is shown in Figure 5. GABA results are shown in Figure 5A-C. Creatine results are shown as a reference in Figure 5D-F. An example of a spectral fit of GABA and creatine is shown in panels A and D respectively. The SNR and the fitting error (CRLB) were determined with different averaging, as shown in the graphs in Figure 5B,C for GABA and E,F for creatine.

The SNR improves with increasing number of averages as expected for both GABA (Figure 5B) and creatine (Figure 5E), and for both *in vivo* and phantom measurements (solid and dotted lines respectively). The goodness of fit results for the *in vivo* measurements (Figure 5C,F) showed that approximately 16 averages are needed to reach a stable fit for GABA, and about eight averages for creatine, as estimated by the required number of averages for the CRLB to reach a plateau. After 16 signal averages, the rate of GABA CRLB decay is less than 10% for all participants. For the phantom measurements, fewer averages (<10) are needed for the CRLB to reach a plateau for both GABA and creatine. The required NSA must be a multiple of two, since one average (NSA 1) either contains an odd or an even editing spectrum. The corresponding scan time for 16 averages is 1 min 23 s; the full 64 averaged editing sets take 5 min 30 s to acquire.

The GABA concentration over time, for three repeated MRS scans in three participants at rest, is shown in Figure 6. The GABA concentration is displayed with reference to creatine, both when averaging consecutive sets of 16 signal averages (Figure 6A), and as a moving average (Figure 6B) with a window of 16 signal averages and a step size of two signal averages. Each data point consists of 16 signal averages, corresponding to a short scan time of 1 min 23 s. Note that, in both graphs, the individual GABA concentration with reference to creatine fluctuates over time for repeated GABA measurements at rest. The observed variability of the GABA over creatine ratios can predominantly be attributed to the variability of the GABA concentrations, since the coefficient of variation (CV) of creatine is on average only 1.4% within scans, and 3.8% between scans (NSA 64). To further assess the size and origin of the GABA fluctuations a bootstrap analysis is performed, determining the stability of the GABA measurements.

**Stability**

The GABA stability results of the repeated spectroscopy measurements are shown in Figure 7. Both six repeated scans in a phantom (Figure 7A,C,E, G) and three repeated scans in three participants (Figure 7B,D,F,H) are displayed. A bootstrap analysis is performed, both for averaging 16 signal

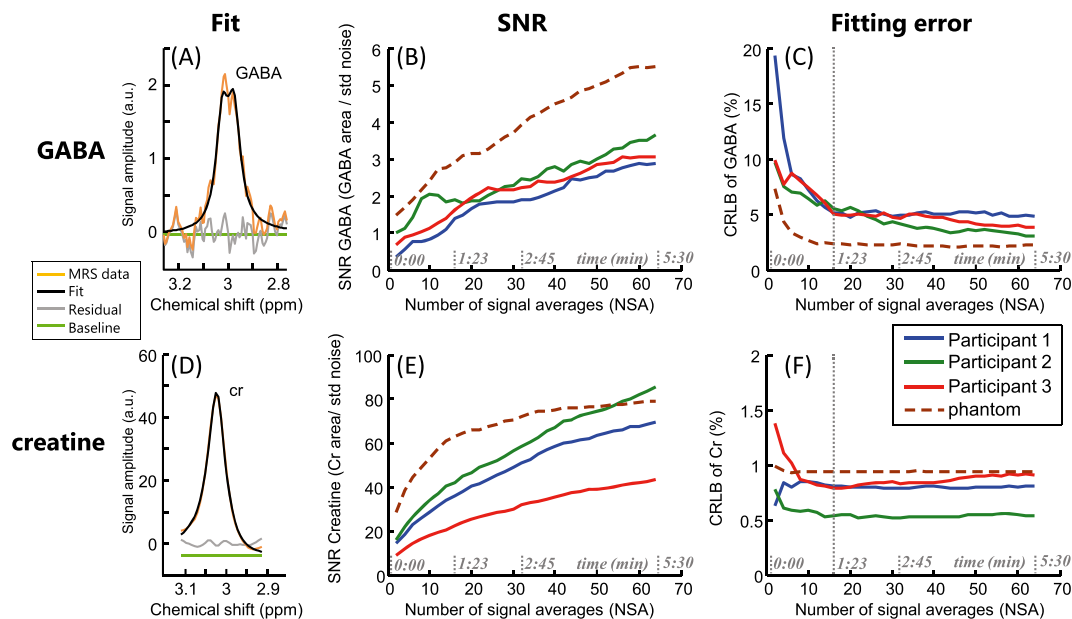


**FIGURE 5** Spectral fitting, SNR, and goodness of fit. (A,D), An example of the spectral fit for both metabolites, GABA and creatine. (B,E), The SNR with different averaging. In all cases, the SNR increases with the number of averages. (C,F), The fitting error, as described by the CRLB. Note that fewer than 16 signal averages (indicated by a vertical dotted line) are needed for the GABA fit to become stable, as estimated by the required number of averages for the CRLB to reach a plateau. After 16 signal averages, the rate of GABA CRLB decay is less than 10% for all participants. The acquisition of 16 signal averages converts to a scan time of less than 1 min 23 s

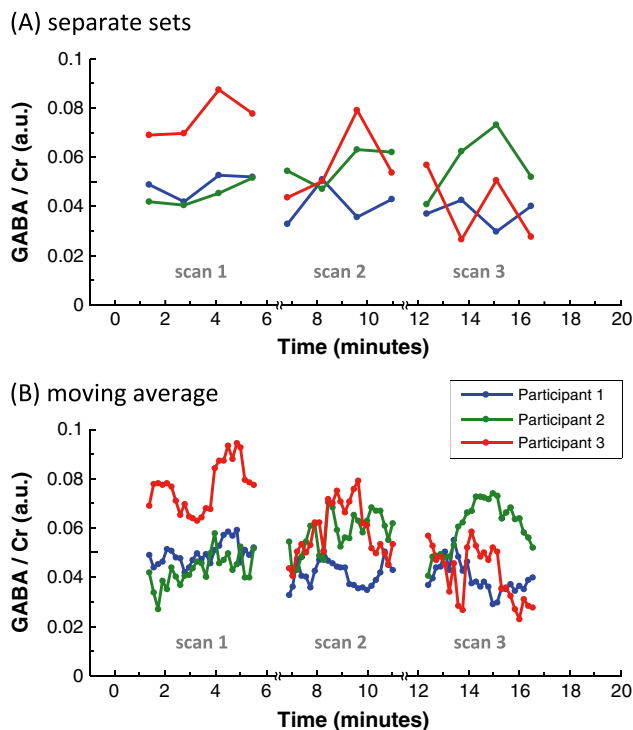


**FIGURE 6** GABA concentration over time referenced to creatine, as measured by three repeated GABA edited spectroscopy scans in three participants at rest. The GABA concentration is displayed (A) when averaging consecutive sets of 16 signal averages, and (B) as a moving average with a window of 16 signal averages and a step size of two signal averages. Each data point consists of 16 signal averages, corresponding to a short scan time for GABA edited spectroscopy of 1 min 23 s. The individual GABA concentration at rest fluctuates over time

averages (Figure 7A-D) and 32 signal averages (Figure 7E-H) out of a total of 64 signal averages. For each data point, the relative metabolite concentration is plotted, as defined by the area under either the GABA (Figure 7, top row) or creatine peak (Figure 7, bottom row). The graphs show the results for the repeated scans separately (six for the phantom, three for each participant). The error bars indicate the mean and SD of the relative GABA or creatine concentrations computed from the 500 fits of the bootstrap procedure. The percentage displayed next to the error bars

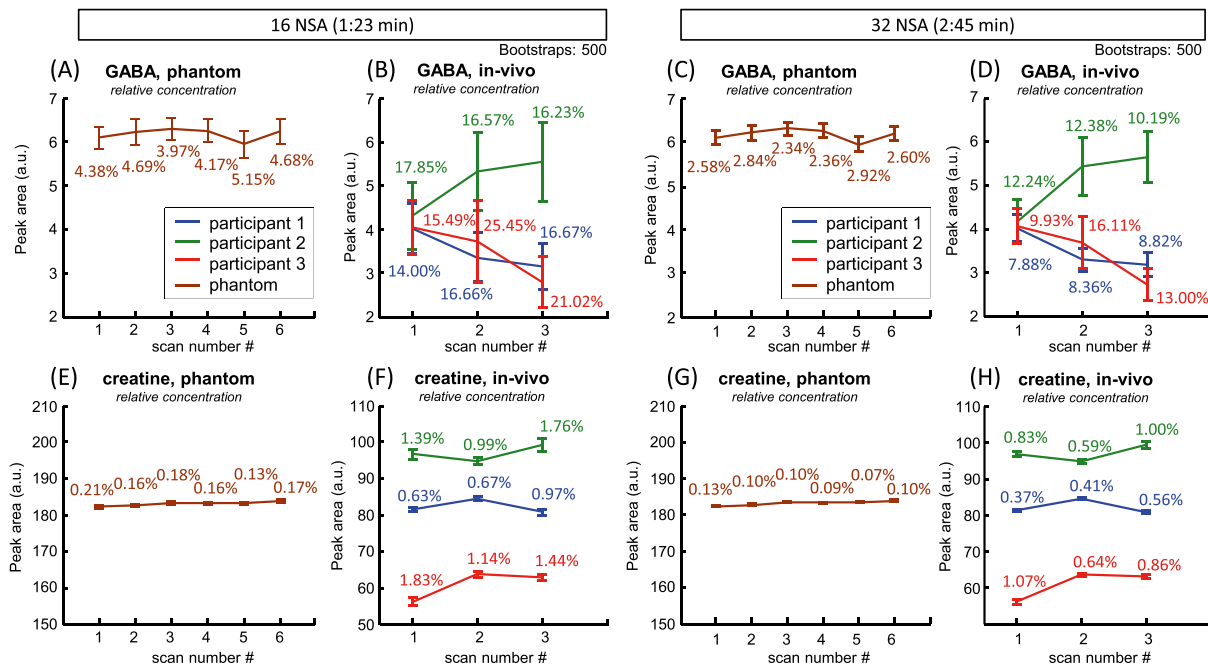


**FIGURE 7** Repeated MRS measurements of GABA (A–D), and creatine (E–H), for the phantom (A,C,E,G), and *in vivo* (B,D,F,H). The graphs show the results for the repeated scans separately (six for the phantom, three for each participant). To estimate the variation of the concentrations per scan, 500 bootstrap fits were performed. Results are shown for spectra consisting of 16 signal averages (A,B,E,F), and 32 signal averages (C,D,G,H). The mean, SD (error bar), and their ratio (percentage) across the 500 estimated GABA and creatine concentrations are shown in the graphs. Despite the same intrinsic SNR of GABA, the *in vivo* levels show, per scan, higher fluctuations (NSA 16, 14–25%; NSA 32, 8–16%) than the phantom results (NSA 16, 5%; NSA 32, 3%)

represents the ratio of SD and the mean. For the phantom, this ratio of the SD and the mean of the measured GABA concentrations is less than 5% for 16 signal averages and less than 3% for 32 signal averages (Figure 7 A,C). For creatine, it is less than 0.5% in both cases (Figure 7 E,G), which is similar to the total system stability. *In vivo*, the ratio of the SD and the mean of the measured GABA concentrations is between 14 and 25% for 16 signal averages and between 8 and 16% for 32 signal averages (Figure 7 B,D). For creatine this is between 0.5 and 2% for both 16 and 32 signal averages (Figure 7 F,H). The variation of GABA is larger than the variation of creatine.

Since the measured metabolite values (Figure 7) are relative concentrations, the ratio of GABA to other metabolites (Table 3 and 4) was also calculated to facilitate comparison with other studies. The GABA ratio is calculated with respect to the reference metabolite, creatine (Table 3), and water (Table 4). The GABA ratios for the three scans per participant are shown in both tables. Also, descriptive information is reported per participant, such as the mean, SD, CV (%), and the absolute difference in terms of percentage (Abs Diff, % defined as the difference between first and last

**TABLE 3** Repeated measurements of GABA concentrations referenced to creatine, using a MEGA-sLASER sequence. The rows indicate the different participants. Columns 2–4 show the measured GABA ratios. The remaining columns show the calculated statistics, characterizing the variation in the GABA measurements

Participant	GABA/cr ( $\times 10^{-2}$ IU)			Mean	SD	CV (%)	Abs Diff (%)
	scan 1	2	3				
1	4.94	3.90	3.95	4.27	0.6	13.7	23.2
2	4.30	5.74	5.68	5.24	0.8	15.6	26.4
3	7.28	5.80	4.34	5.80	1.5	25.3	50.6
Mean						18.2	33.4

**TABLE 4** Repeated measurements of GABA concentrations referenced to water, using a MEGA-sLASER sequence

Participant	GABA/H <sub>2</sub> O ( $\times 10^{-5}$ IU)			Mean	SD	CV (%)	Abs Diff (%)
	scan 1	2	3				
1	4.23	3.45	3.33	3.67	0.5	13.3	24.2
2	4.49	5.73	5.95	5.39	0.8	14.7	27.3
3	4.37	4.04	2.93	3.78	0.8	19.9	38.0
Mean						16.0	29.9

scans, divided by the mean signal for the participant). The last row shows statistics for the average over all participants, reported as the mean CV and mean Abs Diff.

Note that the mean CV over all participants for the GABA measurements is 18% (range 14%-25%) when referenced to creatine and 16% (range 13%-20%) when referenced to water. The mean absolute variation of GABA is 33% (range 23%-50%) referenced to creatine and 30% (range 24%-38%) referenced to water.

## 5 | DISCUSSION

The aim of this study was to reduce scan time and increase GABA sensitivity for edited spectroscopy in the visual cortex. The developed half volume coil setup increased the spatial extent of fMRI activation, enabling an increase voxel size, yielding a gain in GABA SNR by a factor of 2.2 as compared with a conventional head coil setup at 7 T. The gain in SNR can be exchanged for shorter acquisition times. Using this setup and the MEGA-sLASER sequence with FOCI pulses, we were able to obtain a reliable fit of the GABA peak *in vivo* in 1 min 23 s. The stability of the GABA measurements, with the approach employed here, was sufficient to detect GABA with an accuracy of 3% in 2:45 min and 5% in 1 min 23 s, as determined with the GABA phantom. The GABA measurements show larger fluctuations *in vivo* than in the phantom, suggesting the influence of physiological variability. *In vivo*, the concentration changes of GABA measurements were of the order of 18% per participant, which suggests that physiological variability might be substantially higher than the stability of the setup and approach presented.

Our approach involved multiple avenues to enhance GABA MRS sensitivity. A half volume multi-transmit coil was constructed and combined with a large screen for visual stimulation, enabling a projection size, with a visual angle, of more than 60°. As no close fitting volume transmit coil was used,  $B_1$  shimming was performed with the constructed transmit array of the half volume coil. This resulted in a uniform field over the spectroscopy voxel, but also assured sufficient  $B_1^+$  to use the short adiabatic RF pulses, required for the optimized GABA acquisition. GABA MRS signal was acquired with a MEGA-sLASER sequence with macromolecular nulling and FOCI editing pulses to enhance the sensitivity and spatial localization of GABA signals. High density receive surface arrays, which yield a high SNR in the visual cortex for a distance of several centimeters from the coil elements, were used for signal reception. The effectiveness of the constructed setup at 7 T is discussed in more detail below.

### 5.1 | Coil setup performance

The achieved extent of tissue activation in the visual cortex, as measured with fMRI, was larger with the half volume coil setup than with the standard head coil setup, most evidently for V1 (Figure 2C,E). It is expected that this is caused predominantly due to the increased visual angle (larger presentation screen) of the half volume coil setup. The increased activated tissue volume encompassed approximately the whole extent of V1. The increase in active voxels within the voxel ROI was relatively modest, of the order of 19%, likely because other visual areas were also included in the ROI (such as V2 or V3). The difference in spatial extent of activation between setups was translated to 2.8 times larger spectroscopy volumes containing stimulated tissue. The GABA spectroscopy comparison between setups showed a gain in SNR by a factor of 2.2 on average for the half volume coil setup. The increase in GABA SNR arises directly from the increased voxel size, which is possible due to a larger activated cortical volume when using the half volume coil setup. The achieved gain in SNR can be used either to perform measurements with higher GABA sensitivity or to enable shorter measurement times. However, the gain in GABA SNR of 2.2 did not scale linearly with the gain in voxel size of 2.8. This can be expected since the sensitivity profile of the surface receive coils decays towards the center of the brain, and the voxel size was expanded towards the center of the brain. The use of a dedicated coil setup for the back of the brain enhances the SNR close to the coils, but at the same time results in lowered SNR towards the center of the brain.

### 5.2 | SNR, speed, and stability of the GABA measurements

The SNR of the GABA measurements increased with NSA as expected. The goodness of fit of the GABA peak also improved with NSA, as expressed by the CRLB, and became stable in fewer than 16 signal averages, which can be acquired in less than 1 min 23 s. When comparing the 1 min 23 s acquisition time with the 6-30 min typical scan times reported for GABA edited spectroscopy in the literature,<sup>16</sup> an approximate 4 to 20-fold improvement is achieved. However, when compared with the typical fMRI acquisition times of 1-4 s there is still an order of magnitude difference.

The stability and repetition accuracy of the NSA 16 and 32 GABA measurements was 5% and 3% respectively, as determined with a GABA phantom. This 3-5% variability in GABA measurements for the phantom data suggests that GABA changes of at least 3% can be detected within 2 min 45 s and 5% in 1 min 23 s, excluding physiological confounds. Then again, *in vivo*, the variability of the GABA peaks was substantially higher, both within and between repetitive GABA scans in all participants. The intra scan variability in GABA levels (variability within all averages of one scan) ranged from 8 to 16% (NSA 32) and 14-25% (NSA 16) in a period of 5 min 30 s. The inter-scan variability (variation between consecutive scans) is larger (CV 18%, Abs Diff 30%) than the variation within one the scan (8-16% for NSA 32, and 14-25% for NSA 16). The variability of the GABA signals is substantially larger than those caused by intrinsic system noise and measurement instabilities, as assessed by the phantom measurements. The origin of this variability is unclear; however, given the much lower variability observed for the phantom measurements it could be of physiological origin.

Noise and motion of the participant can affect the GABA level variation as well. However, a spectrum of poor quality due to motion of the participant would be averaged out in the bootstrapping procedure, which selects 500 sets of 16 or 32 signal averages from a total of 64 signal averages. Extreme artifacts of a single spectrum (NSA 1) per scan (5 min 30 s) would therefore not have much impact on the results obtained for the *in vivo* measurements. The larger voxel size might increase variability of GABA as well. Anatomically, a larger voxel includes more neurons. A larger pool of active and inactive neurons at different locations could possibly explain the increased physiological variations. In this study, the participants were asked to look at a black presentation screen, but were free to close their eyes as well. This could be an additional factor of variation. The variability of GABA is larger than the variability of creatine, which can be expected since the absolute concentration of creatine is in general almost eight times larger than the concentration of GABA. Therefore, small absolute changes of creatine would be less visible in the large creatine pool. In the case of GABA, small absolute changes would result in a large relative change of the total GABA concentration, since the total GABA concentration is low.

When considering a physiological origin of the observed *in vivo* variability in GABA levels, the results may imply that GABA changes of at least 8-16% may be needed in order to be detected in a functional MRS experiment. The high GABA variability impairs the possibility of detecting evoked GABA fluctuations, questioning the motivation to aim for GABA measurements with a high SNR and a short scan time. However, measurements that are made with event-related paradigms may still benefit, and may be able to identify evoked GABA fluctuations from background variability. Another reason for the observed *in vivo* variability in GABA levels could be that the presumed resting state of the visual cortex during our measurements may not hold for GABA physiology. Consequently, new paradigms may be required to set the brain in resting GABA states in order to assess functionally induced alterations in GABA levels. Our result suggests that physiological alterations in GABA levels can occur within the duration of more common MRS acquisitions that average spectra over 6-30 min. However, further work is needed to confirm assumptions about the source of variability of GABA *in vivo*.

### 5.3 | Methodological considerations

A number of methodological aspects have to be taken into account with respect to the coil setup design. Small surface coils tend to yield the highest SNR within their sensitive area, but their receive sensitivity is not very uniform and decreases with distance from the coils.<sup>41</sup> The high density surface coils used in the present setup allow for high sensitivity and SNR up to at least a 4-5 cm distance from the coil elements.<sup>30,31</sup> In the coil setup design, a choice was made to increase the visual angle by increasing the screen size. However, this approach can be argued. It may be possible to achieve the same visual angle with head coil mountable goggles near the participant's eyes, minimizing the distance between the screen and the eyes of the participant.<sup>42,43</sup> Still, the electronics in the goggles should not interfere with the magnetic field, and the compatibility with a 7 T scanner may be an issue. Another confound of large voxel sizes is the stronger demands on  $B_1$  and  $B_0$  shimming. To resolve this issue we adopted multi-transmit technology in the half volume coil design. However, the limited availability of multi-transmit technology for 7 T systems might be a drawback. In this study,  $B_1$  shimming is performed for each participant individually, which extended the scanning protocol by approximately 10 min. However, when aiming for a short scan protocol it is also possible to fix the transmit channels to one general setting. The spectroscopy scans are acquired with a peak  $B_1$  peak amplitude in accordance with the value found in the  $B_1$  map. If the value is lower than expected, the RF pulse durations in the sequence can become longer. With the current hardware there is still room for  $B_1$  field improvement, as the transmit channels are not yet maximally optimized in amplitude and phase settings. The refocusing RF pulses used in the sequence are adiabatic RF pulses and are therefore less sensitive to  $B_1$  variations. However, the RF pulses used for MRS editing are conventional pulses, which can still be a source of variation. Despite the possible  $B_1$  field non-uniformity because of the large MRS voxels, we do expect it to be stable over time. In this sense, therefore, it does not explain the variations we measure over time. As opposed to  $B_1$  shimming, the  $B_0$  shimming in the visual cortex is hardly compromised, particularly considering the broadened spectral lines of GABA due to inherent  $J$  coupling. Finally, the voxel size is mainly enlarged towards the center of the brain, where the distance from the RF coils is greater. Consequently, the SNR may not linearly scale with the enlargement of the voxels.

### 5.4 | Technical comparison with other studies

Several studies have demonstrated changes in GABA levels between patient populations; however, less is known about short term temporal (minute) GABA level fluctuations in individuals.<sup>16</sup> Repeatability studies that measure GABA over time<sup>44-47</sup> report lower fluctuations in GABA per participant with a CV of 4-12% (mean CV, for GABA plus macromolecules referenced to either water or creatine at 3 T). However, these studies use a MEGA-PRESS sequence, without macromolecular suppression. Macromolecular contamination can have a significant impact on the GABA results.<sup>48,49</sup> Two studies performed at 7 T, which do incorporate macromolecular suppression, show a higher GABA CV of 9.5% and 13.6%,<sup>50,51</sup> with total acquisition times of 12 min 48 s and 8 min respectively. In addition, a recent study performed at 3 T, which includes macromolecular suppression and motion navigation, reports a CV of 13.3-17.6%,<sup>52</sup> with an acquisition time of 10 min 40 s. These values come closer to the CV of GABA variation found in our study of 16%-18%, acquired at 7 T in 5 min 30 s. In our study, we used macromolecular nulled GABA editing techniques, which are obtained with a relatively short total acquisition time. When neglecting consequences of signal overlap, functional GABA MRS acquisitions may be obtained at even higher temporal resolutions using non-edited, short echo time MRS acquisition.<sup>53</sup> Similarly as obtained for functional lactate MRS, these may reveal even faster GABA fluctuations in the visual cortex.<sup>54,55</sup> Despite the short echo time, care must be taken

in assuming constant levels of overlapping resonances and fitting accuracies.<sup>49,56</sup> Short echo time MRS is more heavily dependent on data quality and fitting constraints for the quantification of GABA.<sup>17</sup>

Studies that combine fMRI and GABA MRS are interesting from a fundamental point of view, because they may provide insight into the connection between neuronal metabolism and BOLD hemodynamics. Furthermore, they are also interesting from a clinical point of view, because imbalances in excitatory and inhibitory processes are believed to be implicated in several neuropathological conditions, such as stroke, schizophrenia, autoimmune inflammation, Parkinson's disease, and epilepsy.<sup>7</sup> For the schizophrenia studies that focus on the frontal cortex, the proposed setup with the advantages of a large screen would not be beneficial. However, the application of the setup is widespread, as it can be extended to other brain regions, such as the temporal lobe, where perception of objects and faces is based, which can be impaired in schizophrenia. Or it can be extended to other patient groups, for example neurofibromatosis type 1 patients, in whom a GABA deficit is present in the visual cortex.<sup>57</sup> In both cases our setup can enhance GABA sensitivity or reduce measurement time to approach measurements on a physiological time scale, gaining insight into the diseased brain system.

## 6 | CONCLUSION

The half volume setup enables an increase in the area of visual stimulation, allowing activation of almost the entire V1. Also, more than an average 2.2-fold SNR gain in GABA detection of stimulated tissue can be achieved, as compared with a conventional head coil setup. The SNR, speed, and stability of the sensitivity optimized method employed at 7 T are sufficient to detect GABA with an accuracy of 5%, within a fast scan time of less than 2 min, as determined in a phantom. This brings functional GABA detection at temporal resolutions that match more closely to activation paradigms. However, the repetitive *in vivo* measurements per individual show a large GABA variation of 14–25% at rest, suggesting a physiological origin. Overall, the results indicate new possibilities and considerations for GABA spectroscopy measurements in the field of human brain physiology.

## ACKNOWLEDGEMENT

This work was supported in part by the Netherlands Organization for Scientific Research (NWO) Vidi Grant 13339 (Petridou)

## ORCID

Arjan D. Hendriks  <http://orcid.org/0000-0002-0363-2471>

Catalina S. Arteaga de Castro  <http://orcid.org/0000-0002-1055-2672>

## REFERENCES

1. Kim SG, Ogawa S. Biophysical and physiological origins of blood oxygenation level-dependent fMRI signals. *J Cereb Blood Flow Metab.* 2012;32(7):1188–1206.
2. Ogawa S, Lee TM, Kay AR, Tank DW. Brain magnetic resonance imaging with contrast dependent on blood oxygenation. *Proc Natl Acad Sci U S A.* 1990;87(24):9868–9872.
3. Lauritzen M, Mathiesen C, Schaefer K, Thomsen KJ. Neuronal inhibition and excitation, and the dichotomic control of brain hemodynamic and oxygen responses. *Neuroimage.* 2012;62(2):1040–1050.
4. Logothetis NK. What we can do and what we cannot do with fMRI. *Nature.* 2008;453(7197):869–878.
5. Attwell D, Buchan AM, Charpak S, Lauritzen M, Macvicar BA, Newman EA. Glial and neuronal control of brain blood flow. *Nature.* 2010;468(7321):232–243.
6. Buzsaki G, Kaila K, Raichle M. Inhibition and brain work. *Neuron.* 2007;56(5):771–783.
7. Donahue MJ, Near J, Blicher JU, Jezzard P. Baseline GABA concentration and fMRI response. *Neuroimage.* 2010;53(2):392–398.
8. Logothetis NK, Pauls J, Augath M, Trinath T, Oeltermann A. Neurophysiological investigation of the basis of the fMRI signal. *Nature.* 2001;412(6843):150–157.
9. Muthukumaraswamy SD, Edden RA, Jones DK, Swettenham JB, Singh KD. Resting GABA concentration predicts peak gamma frequency and fMRI amplitude in response to visual stimulation in humans. *Proc Natl Acad Sci U S A.* 2009;106(20):8356–8361.
10. Mangia S, Tkac I, Gruetter R, et al. Sensitivity of single-voxel <sup>1</sup>H-MRS in investigating the metabolism of the activated human visual cortex at 7 T. *Magn Reson Imaging.* 2006;24(4):343–348.
11. Northoff G, Walter M, Schulte RF, et al. GABA concentrations in the human anterior cingulate cortex predict negative BOLD responses in fMRI. *Nat Neurosci.* 2007;10(12):1515–1517.
12. Kuhn S, Schubert F, Mecke R, et al. Neurotransmitter changes during interference task in anterior cingulate cortex: evidence from fMRI-guided functional MRS at 3 T. *Brain Struct Funct.* 2016;221(5):2541–2551.
13. Lipp I, Evans CJ, Lewis C, Murphy K, Wise RG, Caseras X. The relationship between fearfulness, GABA+, and fear-related BOLD responses in the insula. *PLoS ONE.* 2015;10(3):e0120101
14. Michou E, Williams S, Vidyasagar R, et al. fMRI and MRS measures of neuroplasticity in the pharyngeal motor cortex. *Neuroimage.* 2015;117:1–10.
15. Bednarik P, Tkac I, Giove F, et al. Neurochemical and BOLD responses during neuronal activation measured in the human visual cortex at 7 Tesla. *J Int Soc Cereb Blood Flow Metab.* 2015;35(4):601–610.

16. Puts NA, Edden RA. In vivo magnetic resonance spectroscopy of GABA: a methodological review. *Prog Nucl Magn Reson Spectrosc.* 2012;60:29-41.
17. Mullins PG, McGonigle DJ, O'Gorman RL, et al. Current practice in the use of MEGA-PRESS spectroscopy for the detection of GABA. *Neuroimage.* 2014;86:43-52.
18. Cleve M, Gussew A, Reichenbach JR. In vivo detection of acute pain-induced changes of GABA+ and Glx in the human brain by using functional <sup>1</sup>H MEGA-PRESS MR spectroscopy. *Neuroimage.* 2015;105:67-75.
19. Arteaga de Castro CS, Boer VO, Andreychenko A, et al. Improved efficiency on editing MRS of lactate and gamma-aminobutyric acid by inclusion of frequency offset corrected inversion pulses at high fields. *NMR Biomed.* 2013;26(10):1213-1219.
20. Adams DL, Horton JC. Ocular dominance columns: enigmas and challenges. *Neuroscientist.* 2009;15(1):62-77.
21. Sengupta S, Roebroek A, Kemper VG, et al. A specialized multi-transmit head coil for high resolution fMRI of the human visual cortex at 7T. *PLoS ONE.* 2016;11(12):e0165418
22. Adriany G, Gruetter R. A half-volume coil for efficient proton decoupling in humans at 4 Tesla. *J Magn Reson.* 1997;125(1):178-184.
23. Adriany G, Pfeuffer J, Yacoub E, et al. A half-volume transmit / receive coil combination for 7 Tesla applications. *Proc Int Soc Magn Reson Med.* 2001;9:1097
24. Avdievich NI, Peshkovsky AS, Kennan RP, Hetherington HP. SENSE imaging with a quadrature half-volume transverse electromagnetic (TEM) coil at 4T. *J Magn Reson Imaging.* 2006;24(4):934-938.
25. Ballon D, Graham MC, Miodownik S, Koutcher JA. A 64 MHz half-birdcage resonator for clinical imaging. *J Magn Reson.* 1990;90(1):131-140.
26. Fujita H, Braum WO, Shvartsman SM, et al. An optimized open quadrature distributed RF surface coil. Paper presented at: The 6th Annual Meeting of the ISMRM; April 18-24, 1998; Sydney.
27. Peshkovsky AS, Kennan RP, Fabry ME, Avdievich NI. Open half-volume quadrature transverse electromagnetic coil for high-field magnetic resonance imaging. *Magn Reson Med.* 2005;53(4):937-943.
28. Katscher U, Bornert P. Parallel RF transmission in MRI. *NMR Biomed.* 2006;19(3):393-400.
29. Andreychenko A, Boer VO, Arteaga de Castro CS, Luijten PR, Klomp DW. Efficient spectral editing at 7 T: GABA detection with MEGA-sLASER. *Magn Reson Med.* 2012;68(4):1018-1025.
30. Petridou N, Italiaander M, van de Bank BL, Siero JC, Luijten PR, Klomp DW. Pushing the limits of high-resolution functional MRI using a simple high-density multi-element coil design. *NMR Biomed.* 2013;26(1):65-73.
31. Batson MA, Petridou N, Klomp DW, Frens MA, Neggers SF. Single session imaging of cerebellum at 7 Tesla: obtaining structure and function of multiple motor subsystems in individual subjects. *PLoS ONE.* 2015;10(8):e0134933
32. Ledden PJ, Mareyam A, Wang S, van Gelderen P, Duyn J. 32 channel receive-only SENSE array for brain imaging at 7T. Paper presented at: 15th Annual Meeting of the ISMRM; 2007; Berlin.
33. Yarnykh VL. Actual flip-angle imaging in the pulsed steady state: a method for rapid three-dimensional mapping of the transmitted radiofrequency field. *Magn Reson Med.* 2007;57(1):192-200.
34. Cox RW. AFNI: software for analysis and visualization of functional magnetic resonance neuroimages. *Comput Biomed Res.* 1996;29(3):162-173.
35. Cabanes E, Confort-Gouny S, Le Fur Y, Simond G, Cozzone PJ. Optimization of residual water signal removal by HLSVD on simulated short echo time proton MR spectra of the human brain. *J Magn Reson.* 2001;150(2):116-125.
36. Edden RA, Puts NA, Harris AD, Barker PB, Evans CJ. Gannet: a batch-processing tool for the quantitative analysis of gamma-aminobutyric acid-edited MR spectroscopy spectra. *J Magn Reson Imaging.* 2014;40(6):1445-1452.
37. Waddell KW, Avison MJ, Joers JM, Gore JC. A practical guide to robust detection of GABA in human brain by J-difference spectroscopy at 3 T using a standard volume coil. *Magn Reson Imaging.* 2007;25(7):1032-1038.
38. Kreis R. Issues of spectral quality in clinical <sup>1</sup>H-magnetic resonance spectroscopy and a gallery of artifacts. *NMR Biomed.* 2004;17(6):361-381.
39. Cavassila S, Deval S, Huegen C, van Ormondt D, Graveron-Demilly D. Cramér-Rao bounds: an evaluation tool for quantitation. *NMR Biomed.* 2001;14(4):278-283.
40. Davison AC, Hinkley DV. *Bootstrap Methods and their Application.* Cambridge: Cambridge University Press; 1997.
41. Asher KA, Bangarter NK, Watkins RD, Gold GE. Radiofrequency coils for musculoskeletal magnetic resonance imaging. *Top Magn Reson Imaging.* 2010;21(5):315-323.
42. Choubey B, Jurcoane A, Muckli L, Sireteanu R. Methods for dichoptic stimulus presentation in functional magnetic resonance imaging—a review. *Open Neuroimaging J.* 2009;3:17-25.
43. James TW, Gauthier I. Repetition-induced changes in BOLD response reflect accumulation of neural activity. *Hum Brain Mapp.* 2006;27(1):37-46.
44. Bogner W, Gruber S, Doelken M, et al. In vivo quantification of intracerebral GABA by single-voxel <sup>1</sup>H-MRS—how reproducible are the results? *Eur J Radiol.* 2010;73(3):526-531.
45. Near J, Ho YC, Sandberg K, Kumaragamage C, Blicher JU. Long-term reproducibility of GABA magnetic resonance spectroscopy. *Neuroimage.* 2014;99:191-196.
46. O'Gorman RL, Michels L, Edden RA, Murdoch JB, Martin E. In vivo detection of GABA and glutamate with MEGA-PRESS: reproducibility and gender effects. *J Magn Reson Imaging.* 2011;33(5):1262-1267.
47. Evans CJ, McGonigle DJ, Edden RA. Diurnal stability of gamma-aminobutyric acid concentration in visual and sensorimotor cortex. *J Magn Reson Imaging.* 2010;31(1):204-209.
48. Harris AD, Puts NA, Barker PB, Edden RA. Spectral-editing measurements of GABA in the human brain with and without macromolecule suppression. *Magn Reson Med.* 2015;74(6):1523-1529.
49. Terpstra M, Ugurbil K, Gruetter R. Direct in vivo measurement of human cerebral GABA concentration using MEGA-editing at 7 Tesla. *Magn Reson Med.* 2002;47(5):1009-1012.
50. Prinsen H, de Graaf RA, Mason GF, Pelletier D, Juchem C. Reproducibility measurement of glutathione, GABA, and glutamate: towards in vivo neurochemical profiling of multiple sclerosis with MR spectroscopy at 7T. *J Magn Reson Imaging.* 2017;45(1):187-198.

51. Wijtenburg SA, Rowland LM, Edden RA, Barker PB. Reproducibility of brain spectroscopy at 7T using conventional localization and spectral editing techniques. *J Magn Reson Imaging*. 2013;38(2):460-467.
52. Saleh MG, Near J, Alhamud A, Robertson F, van der Kouwe AJ, Meintjes EM. Reproducibility of macromolecule suppressed GABA measurement using motion and shim navigated MEGA-SPECIAL with LCMoDel, jMRUI and GANNET. *Magn Reson Mater Phys Biol Med*. 2016;29(6):863-874.
53. Near J, Andersson J, Maron E, et al. Unedited *in vivo* detection and quantification of  $\gamma$ -aminobutyric acid in the occipital cortex using short-TE MRS at 3 T. *NMR Biomed*. 2013;26(11):1353-1362.
54. Mekte R, Kuhn S, Pfeiffer H, Aydin S, Schubert F, Ittermann B. Detection of metabolite changes in response to a varying visual stimulation paradigm using short-TE  $^1\text{H}$  MRS at 7 T. *NMR Biomed*. 2017;30(2):
55. Mangia S, Garreffa G, Bianciardi M, Giove F, Di Salle F, Maraviglia B. The aerobic brain: lactate decrease at the onset of neural activity. *Neuroscience*. 2003;118(1):7-10.
56. Near J, Simpson R, Cowen P, Jezzard P. Efficient gamma-aminobutyric acid editing at 3T without macromolecule contamination: MEGA-SPECIAL. *NMR Biomed*. 2011;24(10):1277-1285.
57. Violante IR, Ribeiro MJ, Edden RA, et al. GABA deficit in the visual cortex of patients with neurofibromatosis type 1: genotype-phenotype correlations and functional impact. *Brain*. 2013;136(Pt 3):918-925.

**How to cite this article:** Hendriks AD, Fracasso A, Arteaga de Castro CS, et al. Maximizing sensitivity for fast GABA edited spectroscopy in the visual cortex at 7 T. *NMR in Biomedicine*. 2018;31:e3890. <https://doi.org/10.1002/nbm.3890>